

CLOPPA-IPPP Analysis of Electronic Mechanisms of Intermolecular $^1\text{h}J(\text{A,H})$ and $^2\text{h}J(\text{A,D})$ Spin–Spin Coupling Constants in Systems with D–H \cdots A Hydrogen Bonds

Claudia G. Giribet* and Martín C. Ruiz de Azúa

Department of Physics, Facultad de Ciencias Exactas y Naturales, University of Buenos Aires, Ciudad Universitaria, Pab. I, (1428) Buenos Aires, Argentina

Received: June 27, 2005; In Final Form: October 12, 2005

The electronic origin of intermolecular $^2\text{h}J(\text{A,D})$ and $^1\text{h}J(\text{A,H})$ couplings is discussed by means of the CLOPPA-IPPP approach in several model complexes with D–H \cdots A hydrogen bonds. It is found that the origin of these couplings is mainly due to the interaction between the acceptor σ lone pair and vacant molecular orbitals localized in the D–H \cdots A moiety, regardless of the donor and acceptor nuclei. The problem of the larger absolute value of $^2\text{h}J(\text{A,D})$ compared to $^1\text{h}J(\text{A,H})$ is also addressed.

Introduction

The study of hydrogen bonds D–H \cdots A between proximate molecular moieties provides essential information to determine structural conformations of molecular complexes, molecular solids or biological systems. This fact explains the widespread interest that this type of specific interactions has generated among experimental and theoretical researchers. In the past few years, NMR techniques have been applied to obtain structural information about hydrogen bonds, as a complement of the traditional X-ray diffraction spectroscopy. In particular, the experimental measurement of spin–spin couplings between nuclei across hydrogen bonds, first observed in 1998,^{1,2} has become a valuable tool to detect and to characterize hydrogen bonded moieties, specially in biomolecular compounds.^{1–9} Different aspects of this type of couplings have also been analyzed from a theoretical point of view.^{10–37} For example, the existence of such couplings has been related to a covalent character of the hydrogen bonds.^{13,14,16,23,34,35} Correlations between the magnitude of the couplings and structural conformation^{10,13,15,16,18,20–27–32} and strength^{11,12,14,19,21,33,35} of hydrogen bonds were analyzed. An unexpected outcome of both experimental and theoretical studies was that complexes of the type D–H \cdots A can exhibit larger $^2\text{h}J(\text{D,A})$ couplings than $^1\text{h}J(\text{A,H})$ ones (in absolute value).^{2,13,22–26,31,35,37} Attempts to theoretically explain this feature were carried out, within the valence bond order model,¹³ the natural bond orbitals (NBO) analysis,²⁶ and, more recently, the J-OC-PSP method.³⁵

The CLOPPA (contributions from localized orbitals within the polarization propagator approach) method, combined with the IPPP (inner projections of the polarization propagator) technique,^{38–41} is a useful tool to identify the electronic mechanisms operating in a given phenomenon. Many different mechanisms were successfully analyzed by this method at a semiempirical level. In recent years, it was implemented at the ab initio level for the theoretical analysis of NMR spin–spin couplings^{38–44} and the static molecular polarizability tensor.^{25,42,43} It has been applied, for instance, to the analysis of “through-space” couplings in bicyclopentanes,⁴⁴ one-bond couplings in the NH₃ molecule⁴¹ and, more recently, one-bond C–H couplings in complex systems with C–H \cdots O interactions.²⁵

The aim of the present work is to carry out an IPPP–CLOPPA analysis of electronic mechanisms which give rise to $^1\text{h}J(\text{A,H})$ and $^2\text{h}J(\text{A,D})$ spin–spin couplings across a hydrogen bond in a set of small model compounds. Transmission mechanisms are described in terms of “coupling pathways” J_{ij} involving two occupied (i,j) localized molecular orbitals (LMOs), and “coupling pathways” $J_{ia,jb}$ involving two occupied (i,j) and two vacant (a,b) LMOs. The relative importance of different LMOs in the coupling transmission can then be assessed. In first place, a brief account of the IPPP–CLOPPA method is presented. In particular, each J_{ij} coupling pathway is explicitly related to the spin electronic density of an occupied LMO at the site of a given nucleus. Then, the localization of occupied and vacant LMOs is discussed. Localization of vacant LMOs deserves special attention, as the number and type of vacant LMOs depend on the atomic basis set, and no previous analysis of vacant LMOs in a D–H \cdots A hydrogen bond were carried out with the localization method used in this work. Numerical results of the IPPP–CLOPPA analysis of $^1\text{h}J(\text{A,H})$ and $^2\text{h}J(\text{A,D})$ are presented in the Results and Discussion. In particular the unexpected trend that $|^2\text{h}K(\text{D,A})|$ are larger than $|^1\text{h}K(\text{A,H})|$ is analyzed. Interesting insights are found, which complement previous studies with different partition techniques.^{13,26,35}

Method

IPPP and CLOPPA Methods. Since the IPPP (inner projections of the polarization propagator approach) and CLOPPA (contributions from localized orbitals within the polarization propagator approach) methods were presented previously,^{38–41} their main ideas are briefly outlined here.

Within the polarization propagator (PP) formalism,⁴⁵ any component of the spin–spin coupling constant between nuclei N and M can be expressed as:³⁸

$$J(\text{N,M}) = \Omega \sum_{ia,jb} V_{ia}(\text{N}) P_{ia,jb} V_{jb}(\text{M}) \quad (1)$$

where Ω is a constant which depends on the interaction considered and contains, among others, the gyromagnetic factors of nuclei N and M; i,j (a,b) indices stand for the occupied i,j (vacant a^*,b^*) molecular orbitals (MOs) of a Hartree–Fock (HF) reference state; $P_{ia,jb}$ is the PP matrix element connecting

* Corresponding author. E-mail: giribet@df.uba.ar.

“virtual excitations” $i \rightarrow a^*$ and $j \rightarrow b^*$. The PP in eq 1 can be evaluated at different levels of approximation: RPA, SOP-PA,^{46,47} etc. In the present work, the analysis is carried out at the RPA level. $V_{ia}(N)$ represents the matrix element of the perturbative Hamiltonian between MOs i and a^* centered at nucleus N, which, for the Fermi contact (FC) interaction is given by

$$V_{ia}(N) = \langle i | \delta(\vec{r} - \vec{R}_N) | a^* \rangle \quad (2)$$

and a similar definition stands for $V_{jb}(N)$. These elements are dubbed “perturbators”. The coupling constant $J(N,M)$ can be rewritten in terms of localized MOs (LMOs) by applying to the PP matrix elements and to the perturbators a convenient transformation from canonical HF MOs to occupied and vacant LMOs.³⁹ If the latter are obtained by means of a unitary transformation, the formal expression of $J(N,M)$, eq 1, is not altered and the only difference stands in that i, a, j, b indices now represent LMOs. A four-indices term involving two virtual excitations $i \rightarrow \alpha^*$ and $j \rightarrow \beta^*$ is defined as

$$J_{i\alpha, j\beta} = \begin{cases} (V_{i\alpha}(N)V_{j\beta}(M) + V_{j\beta}(N)V_{i\alpha}(M))P_{i\alpha, j\beta} & i\alpha \neq j\beta \\ V_{i\alpha}(N)V_{j\beta}(M)P_{i\alpha, j\beta} & i\alpha = j\beta \end{cases} \quad (3)$$

Within ab initio calculations and the localization technique⁴¹ applied in this work, there are several vacant LMOs contained in a given local fragment. As will be explained in the following section, local fragments can be defined in such a way that they represent chemical functions like bonds, lone pairs, and atomic inner shells, in the case of occupied LMOs, and antibonds or “anti lone pairs”, for vacant LMOs. If the indices a and b identify these vacant local fragments, it is useful to define the corresponding four-indices term as

$$J_{i\alpha, j\beta} = \sum_{\substack{\alpha \in 'a' \\ \beta \in 'b'}} J_{i\alpha, j\beta} \quad (4)$$

where α (β) represent vacant LMOs of the a^* (b^*) type. This kind of term is called a four-indices coupling pathway.

For a given pair of occupied LMOs i and j , a two-indices coupling pathway can be defined by summing over the whole set of vacant LMOs:

$$J_{ij} = \sum_{a,b} J_{i\alpha, j\beta} \quad (5)$$

Two and four-indices coupling pathways can be useful tools to identify transmission mechanisms of J couplings in terms of local fragments of the electronic distribution. This is the aim of the CLOPPA method.^{39–41} On one hand, perturbators V_{ia} depend on the perturbative interaction under study and reflect the strength of the $i \rightarrow a^*$ virtual excitation. PP matrix elements are perturbation independent: they reflect to what extent two virtual excitations are connected by interactions within the molecular system. From the analysis of these constituent elements, it can be concluded that four-indices coupling pathways can be considered to describe the importance of virtual excitations $i \rightarrow a^*$ and $j \rightarrow b^*$ to transmit the spin information associated, in this case, to the FC interaction.

On the other hand, two-indices coupling pathways J_{ij} allow the following interpretation.⁴¹ Consider an FC-like operator V_j^M which connects the j occupied LMO with the vacant LMOs (b^*) at the site of nucleus M:

$$V_j^M = \sum_b^{\text{vac}} \langle b^* | \delta(\vec{r} - \vec{R}_M) | j \rangle (b^+ j + j^+ b) = \sum_b^{\text{vac}} V_{jb}(M) (b^+ j + j^+ b) \quad (6)$$

where in this equation, b^+ (b) represents a creation (annihilation) operator which creates (annihilates) an electron in a b LMO. A similar explanation stands for j^+ (j). In the presence of this perturbative operator, the i occupied LMO is modified in such a way that it now has contributions from vacant LMOs. The modified $|i^M\rangle$ LMO can be expressed as

$$|i^M\rangle = |i\rangle + \sum_a^{\text{vac}} \sum_b^{\text{vac}} P_{ia, jb} V_{jb}(M) |a^*\rangle \quad (7)$$

The electronic density of the perturbed i LMO at the nucleus N site, $|\tilde{\psi}_i^M(N)|^2$, due to the LMO j perturbed at the M nucleus site, results, up to second order in V:

$$|\tilde{\psi}_i^M(N)|^2 = \langle i^M | \delta(\vec{r} - \vec{R}_N) | i^M \rangle \cong \langle i | \delta(\vec{r} - \vec{R}_N) | i \rangle + 2 \sum_a^{\text{vac}} \sum_b^{\text{vac}} P_{ia, jb} V_{ia}(N) V_{jb}(M) \quad (8)$$

Taking into account that J_{ij} is calculated as

$$J_{ij} = \Omega \sum_a^{\text{vac}} \sum_b^{\text{vac}} P_{ia, jb} (V_{ia}(N)V_{jb}(M) + V_{ia}(M)V_{jb}(N)) \quad (9)$$

where Ω is a negative constant, each term J_{ij} is proportional to

$$J_{ij} \propto -\frac{1}{2} \{ [|\tilde{\psi}_i^M(N)|^2 - |\psi_i(N)|^2] + [|\tilde{\psi}_j^M(N)|^2 - |\psi_j(N)|^2] \} \quad (10)$$

where $\psi_i(N)$ is the unperturbed LMO i evaluated at the N nucleus site (similar definitions stand for the other symbols). Following a similar reasoning, J_{ij} can also be expressed as

$$J_{ij} \propto -\frac{1}{2} \{ [|\tilde{\psi}_i^M(N)|^2 - |\psi_i(N)|^2] + [|\tilde{\psi}_i^N(M)|^2 - |\psi_i(M)|^2] \} \quad (11)$$

where in this last equation, it is taken into account that the perturbation has connected the LMO j with vacant LMOs at the M nucleus site, in the first bracket, and at the N nucleus site, in the second one. Equations 10 and 11 allow the following interpretations of J_{ij} :⁴²

(a) The sum of electronic density changes of LMOs i and j at the site of one nucleus when LMO j and i are perturbed at the other nucleus, respectively.

(b) The sum of electronic density changes of LMO i at both nuclei sites when LMO j is perturbed at the other nucleus site.

Although i, j are the only LMOs to appear explicitly in each two-indices coupling pathways, J_{ij} , and i, a^*, j, b^* , the only ones in $J_{ia, jb}$, it must be emphasized that the influence of the rest of the spin polarized LMOs is also present through the PP matrix element $P_{ia, jb}$. Hence, if the contribution to the coupling transmitted strictly through a fragment L defined by a subset of occupied and vacant LMOs is sought, J^L , it can be defined using the IPPP technique as:^{38–41}

$$J^L = \sum_{ia \geq jb \in L} J_{ia, jb}^L \quad (12)$$

where $J_{ia,jb}^L$ is calculated as in eq 3, but now the PP element is obtained by inner-projecting the full PP matrix on the set of virtual excitations among LMOs within the molecular fragment L. In this way, electrons which do not belong to the molecular fragment L are not allowed to be spin-polarized neither by direct interaction with the nuclei, nor by Coulomb interactions with the polarized electrons in L. J^L is dubbed the “local” contribution to the coupling transmitted through the fragment L. The contribution transmitted by the rest of the molecule, J^R , can be determined as

$$J^R = J - J^L \quad (13)$$

Finally, the indirect influence of the rest of the LMOs, which do not belong to L, on coupling pathways within L can be estimated as

$$J_{\text{ind}}^L = \sum_{ia \geq jb \in L} J_{ia,jb} - J_{ia,jb}^L \quad (14)$$

where the first term of eq 14 is calculated with the full PP matrix. It is noteworthy that, as perturbators in each term of the sum in eq 14 are the same, this quantity describes how much LMOs other than those which belong to L, contribute to define the magnitude of the PP matrix elements associated with virtual excitations within L.

Localization Technique. The localization technique used in this work is Engelmann’s,⁴⁰ applied in an iterative way. With this method, occupied and vacant MOs from an ab initio RHF calculation can be transformed to yield LMOs which closely resemble the chemical picture of bonds, lone pairs, inner shells, and their corresponding vacant LMOs (antibonds, anti lone pairs, etc.). To obtain LMOs, each local fragment is defined by a subset of atomic orbitals (AOs). LMOs within the local fragment are obtained as combinations of MOs with maximum orthogonal projection over the subset of AOs that define the fragment. The only constraint required is that the transformation applied preserves the orthonormality of the LMOs thus obtained (unitary transformation). This procedure is applied separately to occupied and vacant MOs. Occupied LMOs are classified as atom X inner-shells $S(X)$, bonding orbitals X–Y (σ and π types) and X atom lone pairs, LP(X).

Localization of vacant LMOs is a difficult task since the number and type of LMOs depend on the basis set used. For example, the number of vacant MOs obtained in the present calculations are approximately from 100 to 140 MOs, while occupied MOs are around 10 to 14 MOs. The criterion adopted in the present work to define the set of vacant LMOs from the canonical MOs is the following. The localization procedure over a selected fragment L consists of two steps: (i) the localization technique is applied using the orthogonal projector associated with L and the transformed vacant MOs with eigenvalues near 1.0 or, if appropriate, of the same order as the eigenvalue of the corresponding occupied LMO, are retained; (ii) the retained MOs are localized again, using the orthogonal projector built with the subset of AOs complementary to L. From this newly transformed set of MOs obtained in this second step those with smallest eigenvalues can be considered to be simultaneously within L and almost orthogonal to the rest of the system. Again, the criterion to set the threshold for the smallest projection eigenvalue is to match the occupied LMO corresponding eigenvalue, if any. This procedure was applied in the following order to all systems studied. First, a set of “polarization” LMOs was sought, which correspond to the eigenfunctions of a projector made up with the polarization AOs (3 p-type AOs

per H and 6 d-type AOs per heavier atom). These kind of LMOs are spatially spread over the whole system, but it was already shown⁴² that, although they are important in the Hartree–Fock calculation, they play an almost negligible role in the coupling transmission and therefore can be excluded from the perturbative calculation. It is noteworthy that they are essentially combinations of canonical MOs of highest orbital energies. Then, π -type MOs were localized. The remaining σ -type vacant MOs were localized in the following order. First, one center vacant LMOs were defined as those having maximum projection on the set of AOs centered at a given nucleus X. They are identified, matching the occupied LMOs classification, as $S(X)^*$ when they are of pure s-type, $LP(X)^*$ when they are of s–p–d-type or $LP\pi(X)^*$ when they are of pure p-type. Second, two-center vacant LMOs were defined between directly bonded atoms. They are identified as X–Y*. However, there were several MOs that could not be localized in this way. It was found that they correspond to three-center LMOs localized in the hydrogen bond region D–H...A. It is noteworthy that this type of vacant LMOs, which could be called “bridge vacant LMOs”, arises from vacant canonical MOs of low orbital energies. This fact shows that this type of vacant LMOs are not “supernumerary”, but they have a physical sense in the complex formation. As will be seen in the subsequent sections, these type of vacant LMOs and those of the LP(A)* type, play a fundamental role in the intermolecular coupling transmission. For this reason, these “bridge vacant LMOs” and LP(A)* ones were joined in a single classification, as HB* vacant LMOs, taking into account that LP(A)* are also localized in the hydrogen bond zone.

Results and Discussion

Calculations were carried out for the following nine complexes: NCH...OH₂, NCH...NCH, NCH...FH; FH...OH₂, FH...NCH, FH...FH, CNH...OH₂, CNH...NCH, and CNH...FH. In all cases, atoms of the donor molecule are identified with an index “1”, and those of the acceptor one with an index “2”. D and A stand for the donor and acceptor nuclei, respectively. For all systems considered, geometry optimizations were carried out with the GAUSSIAN program,⁴⁹ adopting a linear configuration in order to simplify the analysis. Calculations of J couplings were carried out at both RPA and SOPPA levels in order to assess the importance of correlation effects. To this end, the SYSMO^{50–52} and DALTON⁵³ programs were used. Only Fermi contact (FC) terms are considered, as this contribution is the dominant one. CLOPPA and IPPP decompositions of J couplings were carried out at the RPA level with a modified version of the SYSMO program. The AO basis set used in all cases is Van Duijneveldt’s (13s7p1d,8s1p)–[13s5p1d,5s1p].⁵⁴ To establish a comparison among them, the reduced coupling constants K and their corresponding two and four indices coupling pathways were calculated. These terms are called, hereafter, K_{ij} and $K_{ia,jb}$, respectively.

In Table 1, total RPA and SOPPA values of ${}^{2h}K(D,A)$ and ${}^{1h}K(A,H)$ are displayed. Values from other works are also shown. However, a quantitative agreement is not to be expected as different geometries were used in some cases, and therefore, a direct comparison cannot be established.

From Table 1 it can be seen that, although correlation effects are important, RPA values follow similar trends than SOPPA ones. In fact, although RPA values are overestimated, the relative relation between ${}^{2h}K(D,A)$ and ${}^{1h}K(A,H)$ are well reproduced by RPA values. Therefore, it can be concluded that RPA values are adequate for performing a qualitative analysis of the main electronic mechanisms involved in both intermo-

TABLE 1: Total RPA and SOPPA Values of ${}^{2h}K(D,A)$ and ${}^{1h}K(A,H)$ for All Complexes Considered (All Values Given in $10^{19} \text{ N A}^{-2} \text{ m}^{-3}$)

| | ${}^{2h}K(D,A)$ | | | ${}^{1h}K(A,H)$ | | |
|-----------|-----------------|-------|--------------------|-----------------|-------|--------------------|
| | RPA | SOPPA | other works | RPA | SOPPA | other works |
| NCH...OH2 | 4.92 | 3.80 | 3.12 ^a | -0.58 | -0.32 | |
| NCH...NCH | 3.80 | 2.64 | 3.54 ^b | -0.42 | -0.21 | |
| NCH...FH | 3.60 | 2.59 | 1.66 ^b | -0.43 | -0.24 | |
| FH...OH2 | 3.32 | 2.24 | 2.14 ^b | -1.57 | -0.95 | |
| FH...NCH | 2.68 | 1.77 | 2.74 ^c | -1.10 | -0.56 | |
| FH...FH | 0.11 | -0.40 | -0.30 ^d | -0.99 | -0.66 | -0.38 ^g |
| CNH...OH2 | 8.85 | 7.28 | 7.70 ^e | -0.84 | -0.49 | |
| CNH...NCH | 10.83 | 6.51 | 7.65 ^f | -0.95 | -0.38 | -0.43 ^f |
| CNH...FH | 4.38 | 3.54 | | -0.53 | -0.37 | |

^a Taken from ref 14, for C₂H₂...OH₂. ^b Taken from ref 14. ^c Taken from ref 28. ^d Taken from ref 32. ^e Taken from ref 11. ^f Taken from ref 18; other values for 2h-coupling: 6.60 (from ref 12), 6.72 (from ref 11), 8.40 (experimental value for Adenine-Thimine base pair, ref 17). ^g Taken from ref 31. All values correspond to FC terms.

lecular couplings, and the origin of the difference between them as well. It is noteworthy that $|{}^{2h}K(D,A)|$ are larger than $|{}^{1h}K(A,H)|$ for all complexes considered, except for (linear) FH...FH, for which the ${}^{2h}K(F1,F2)$ coupling takes a very small value. The analysis of the electronic mechanisms which originate these couplings and, in particular, the origin of the trend mentioned above is performed by means of the CLOPPA approach, taking into account two indices, K_{ij} , and four indices, $K_{ia,jb}$, coupling pathways.

Two Indices ${}^{2h}K_{ij}(D,A)$ and ${}^{1h}K_{ij}(A,H)$ Contributions. In Tables 2 and 3, the main K_{ij} terms (i,j , occupied LMOs) are displayed for all complexes considered, for ${}^{2h}K$ and ${}^{1h}K$, respectively. The direct influence of HB* vacant LMOs is also shown, by calculating the K_{ij} terms excluding the $K_{ia,jb}$ terms which contain at least one vacant HB* LMO.

The following considerations are noteworthy. From Tables 2 and 3 it is seen that couplings through hydrogen bonds are mainly originated in a) the spin polarization of occupied LMOs like lone pairs attached both to D and A, and other occupied LMOs belonging to the D electronic environment, specifically D-H bonds, and (b) the presence of HB* vacant LMOs,

localized in the bridge zone. As it was already mentioned, vacant HB* LMOs seem to be a direct consequence of complex formation, and they involve vacant canonical MOs of low orbital energies. This last fact favors virtual excitations to this type of vacant LMOs, which therefore play a fundamental role in the transmission of the spin information, behaving as "links" between both molecules.

The preceding considerations are referred to the direct influence of HB* LMOs in the K_{ij} terms, eq 5. However it must be recalled that all remainder LMOs of the molecule also affect each K_{ij} contribution, since the PP element takes into account the interaction of the i and j LMOs with all the spin-polarized electronic distribution. To deepen the analysis of the role played by HB* LMOs in the coupling transmission, an IPPP calculation was carried out, where the PP was inner-projected onto all LMOs except those corresponding to HB* ones. The corresponding results for ${}^{1h}K$ and ${}^{2h}K$ are shown in Table 4 as ${}^{1h}K^L$ and ${}^{2h}K^L$. K^L involves coupling pathways $K_{ia,jb}$ where (i) both a and b indices are different from HB* and (ii) the indirect influence of HB* in the PP matrix elements of such coupling pathways is ignored. In the same table, the corresponding indirect contributions, obtained as indicated in eq 14, are labeled K_{ind}^L .

It is observed that HB* LMOs are of crucial importance in the spin information transmission through the hydrogen bond, as all couplings (and all coupling pathways as well) fall off to values near zero when HB* LMOs are excluded from the calculation. Moreover, they mainly participate in a direct way in the coupling transmission, as K_{ind}^L values, which take account of the indirect influence of HB* LMOs yield small contributions to the total couplings. The indirect contribution of HB* LMOs is, in all cases, comparable to the direct one of the rest of the LMOs itself. This is particularly important for complexes with CNH as donor molecule.

From Tables 2 and 3, the following comments are noteworthy on the role of occupied LMOs. As it can be expected, all significant K_{ij} terms for ${}^{2h}K(D,A)$ involve the LP(A) LMO, no matter the type of acceptor molecule involved. The leading terms are those involving this LMO and LMOs of the D electronic surrounding. There is one term of this type for ${}^{2h}K(C1,A)$ and

TABLE 2: Main ${}^{2h}K_{ij}$ Terms and Direct Influence of Vacant LMOs of the HB* Type (no HB*^a), for All Complexes (All Values Given in $10^{19} \text{ N A}^{-2} \text{ m}^{-3}$)

| i | j | NCH...OH ₂ | | NCH...NCH | | NCH...FH | |
|-------|-------------------|-----------------------|---------------------|-----------|---------------------|----------|---------------------|
| | | total | no HB* ^a | total | no HB* ^a | total | no HB* ^a |
| LP(A) | C-H | 2.52 | -0.38 | 1.94 | -0.30 | 2.29 | 0.06 |
| LP(A) | LP(A) | 0.72 | -0.18 | 0.90 | -0.75 | 0.52 | 0.28 |
| LP(A) | A-X2 ^b | 0.89(×2) | -0.09(×2) | 0.78 | -0.33 | 0.36 | ~0.00 |
| i | j | FH...OH ₂ | | FH...NCH | | FH...FH | |
| | | total | no HB* ^a | total | no HB* ^a | total | no HB* ^a |
| LP(A) | LP(F1) | 4.14 | 0.40 | 3.58 | 0.97 | 1.75 | 0.37 |
| LP(A) | F1-H | -1.89 | -0.17 | -1.55 | -0.09 | -1.09 | -0.20 |
| LP(A) | S(F1) | -1.89 | -0.20 | -1.55 | -0.40 | -1.15 | -0.24 |
| LP(A) | LP(A) | 0.71 | 0.20 | 1.03 | -0.22 | 0.17 | 0.16 |
| LP(A) | A-X2 ^b | 0.74(×2) | 0.01(×2) | 1.10 | -0.14 | 0.29 | 0.12 |
| i | j | CNH...OH ₂ | | CNH...NCH | | CNH...FH | |
| | | total | no HB* ^a | total | no HB* ^a | total | no HB* ^a |
| LP(A) | LP(N1) | 5.63 | 0.27 | 9.15 | 0.74 | 3.27 | 0.38 |
| LP(A) | LP(A) | 0.71 | 0.21 | 1.72 | 0.18 | 0.30 | 0.09 |
| LP(A) | A-X2 ^b | 0.58(×2) | -0.05(×2) | 1.54 | 0.15 | 0.34 | 0.08 |

^a No HB* stands for contributions obtained excluding the $K_{ia,jb}$ terms which contain at least one vacant HB* LMO from the K_{ij} term calculation.

^b X2 stands for the atom directly bonded to the A atom.

TABLE 3: Main ${}^1hK_{ij}$ Terms and Direct Influence of Vacant LMOs of the HB* Type (no HB*^a), for All Complexes (All Values Given in $10^{19} \text{ N A}^{-2} \text{ m}^{-3}$)

| <i>i</i> | <i>j</i> | NCH...OH ₂ | | NCH...NCH | | NCH...FH | |
|----------|----------|-----------------------|---------------------|-----------|---------------------|----------|---------------------|
| | | total | no HB* ^a | total | no HB* ^a | total | no HB* ^a |
| LP(A) | C1-H | -0.54 | 0.15 | -0.44 | -0.16 | -0.43 | 0.13 |
| <i>i</i> | <i>j</i> | FH...OH ₂ | | FH...NCH | | FH...FH | |
| | | total | no HB* ^a | total | no HB* ^a | total | no HB* ^a |
| LP(A) | F1-H | -1.42 | -0.08 | -1.13 | -0.09 | -0.83 | -0.06 |
| <i>i</i> | <i>j</i> | CNH...OH ₂ | | CNH...NCH | | CNH...FH | |
| | | total | no HB* ^a | total | no HB* ^a | total | no HB* ^a |
| LP(A) | N1-H | -0.53 | 0.05 | -0.68 | -0.02 | -0.36 | 0.20 |
| LP(A) | LP(N1) | -0.25 | 0.02 | -0.40 | ~0.00 | -0.14 | 0.05 |

^a No HB* stands for contributions obtained excluding the $K_{ia,jb}$ terms which contain at least one vacant HB* LMO from the K_{ij} term calculation.

TABLE 4: IPPP Calculated Values Excluding the HB* LMOs (K^L) and Indirect Contribution (as defined in Eq 14) of the HB* LMOs (K_{ind}^L) (All Values Given in $10^{19} \text{ N A}^{-2} \text{ m}^{-3}$)

| | ${}^{2h}K(A,D)$ | | ${}^{1h}K(A,H)$ | |
|-----------------------|-----------------|--------------------|-----------------|--------------------|
| | ${}^{2h}K^L$ | ${}^{2h}K_{ind}^L$ | ${}^{1h}K^L$ | ${}^{1h}K_{ind}^L$ |
| NCH...OH ₂ | -0.12 | -0.26 | 0.03 | 0.00 |
| NCH...NCH | -0.02 | -0.25 | 0.00 | -0.14 |
| NCH...FH | -0.17 | 0.47 | 0.04 | 0.09 |
| FH...OH ₂ | 0.19 | 0.31 | -0.08 | -0.03 |
| FH...NCH | 0.27 | -0.19 | -0.07 | -0.08 |
| FH...FH | -0.09 | 0.41 | -0.09 | 0.03 |
| CNH...OH ₂ | 0.23 | 0.83 | -0.01 | 0.08 |
| CNH...NCH | 0.61 | 0.79 | -0.02 | 0.01 |
| CNH...FH | 0.09 | 0.53 | 0.03 | 0.25 |

${}^{2h}K(N1,A)$ (with C1-H in the former and LP(N1) in the latter), yielding the largest individual contribution. In the case of ${}^{2h}K(F1,A)$ there are three terms of this type, namely, those which involve LP(A) and LP(F1), F1-H or S(F1). However, rather unexpectedly, these three leading terms nearly cancel each other (see Table 2) for all acceptors A considered. As a consequence, ${}^{2h}K(F1,A)$ is defined by other terms of smaller magnitude. This odd behavior can be explained if the interpretation of K_{ij} terms, eqs 10 and 11, is taken into account and the following rationalization is made. When electrons in LP(A) LMO are magnetically perturbed at the A nucleus, occupied LMOs of the F1 surroundings (S(F1), F1-H, and LP(F1)) are modified, yielding partial occupation of vacant LMOs. However, it is observed that the s electronic density of all three perturbed LMOs added together is almost the same as the that of the unperturbed LMOs. Parts a-c of Figure 1 depict these features. The total (Figure 1a), s (Figure 1b), and non s (Figure 1c) electronic density differences between perturbed and unperturbed LMOs of the FH molecule in FH...OH₂ are shown. This effect explains the partial cancellation of the main three K_{ij} terms in complexes where FH is the donor molecule.

No LMOs of the donor C1 surrounding other than C1-H yield large contributions. N-C1 and S(C1) LMOs are hardly affected. In the CNH case, the large K_{ij} term ($i = LP(N1)$, $j = LP(A)$) is explained as essentially due to the spin perturbation of the LP(A) LMO at the site of the acceptor A nucleus, largely affecting LP(N1). The LP(N1) charge density diminishes in a large amount at the N1 site when compared with the unperturbed LMO. Figure 2 shows the characteristics of CNH...OH₂ and NCH...OH₂. It is noteworthy that in all cases considered,

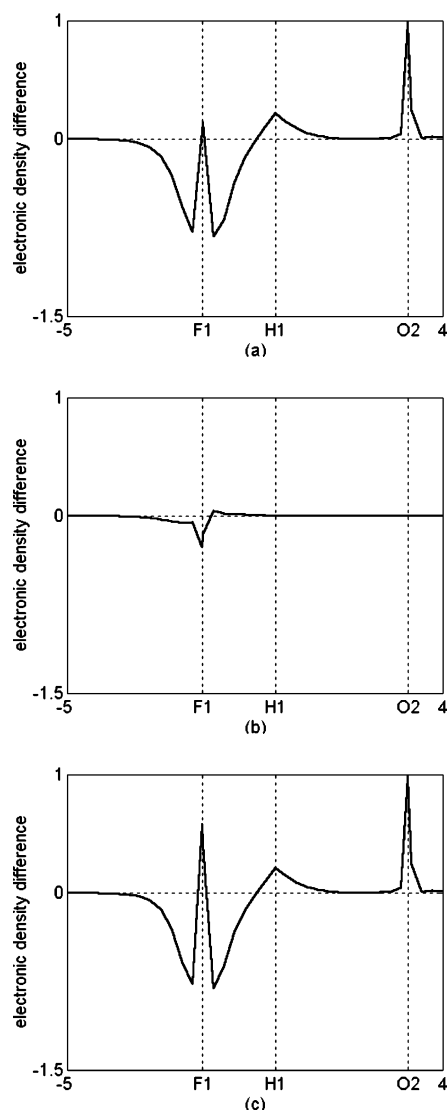


Figure 1. Sum of electronic density differences (in au) among perturbed and unperturbed LMOs of the FH molecule (F1-H, LP(F1) and S(F1)), due to the spin perturbation of LP(O2) at the O2 site, in the FH...OH₂ complex. Key: (a) total density change; (b): density change of s character; (c): density change of non s character.

perturbed D-H LMOs have the largest contributions from vacant LMOs of the D atom surrounding, and from HB* vacant LMOs.

This different behavior of K_{ij} terms mentioned above can be explained as follows. Such K_{ij} terms can be thought of as the response of LMOs of the donor D environment due to the magnetic perturbation of LP(A) at the A nucleus, i.e., only one electronic density difference of eq 10 is significant. The response of a given LMO depends on its shape, orbital energy and neighboring vacant LMOs. For instance, atoms bearing σ -type lone pairs have a reduced s-character of bonds. This is the case of F1-H and N1-H, in opposition to C1-H, which has a large s-character. Similarly, it is observed that the s-character of antibonds and HB* vacant LMOs is reduced at the donor F and N sites when compared to the case of donor C. This effect could be ascribed to the presence of vacant LMOs related to a single atom, as anti lone pairs. As a consequence, perturbators which involve bonds and antibonds or bonds and HB* are much smaller for donor F or N atoms than those corresponding to donor C one. The perturbed D-H electronic density at the D atom is significant when the LMO "mixes" with local vacant

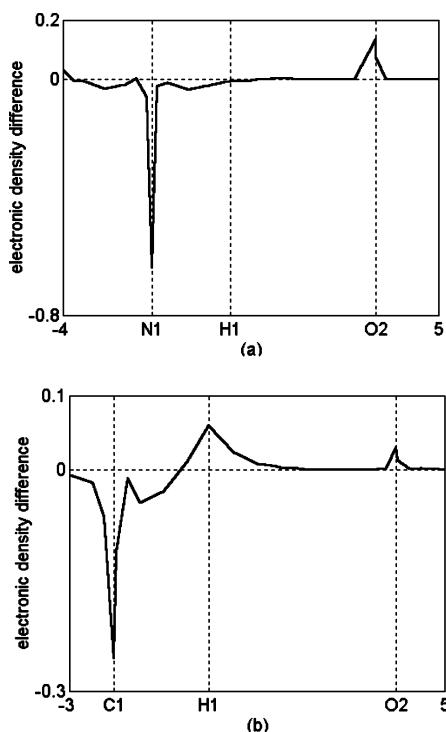


Figure 2. Electronic density difference (in au) among perturbed and unperturbed LMOs. Key: (a) LP(N1), due to the spin perturbation of LP(O2) at the O2 site, in the CNH...OH₂ complex. (b): C1-H, due to the spin perturbation of LP(O2) at the O2 site, in NCH...OH₂.

LMOs, as S(D)* or LP(D)*. Density changes at the A nucleus arise from contributions due to HB* LMOs. On these grounds, it may be concluded that C1-H is the LMO yielding efficient coupling transmission for D = C1, and LP(D) is the one in the case D = N1, as these LMOs have large *s*-character. The σ -type N1-C1 and S(C1) LMOs, and C1-N1 and S(N1) ones, in the first and second cases, play no role in the coupling transmission. However, in D = F1, all three S(F1), F1-H, and LP(F1) LMOs yield non negligible coupling terms. Perturbed LP(F1) and S(F1) do not extend out of the F1 surroundings. They mix only with S(F1)* and LP(F1)* LMOs. As HB* LMO has a reduced *s*-character at the F1 nucleus, the F1-H perturbed LMO has also its largest contributions from S(F1)* and LP(F1)* at the F1 site. The sum of these effects leads to the cancellation of electronic density changes mentioned above. Density changes at other nuclei sites (particularly, at the O2 site) arise from contributions due to HB* LMOs, mainly via p-type AOs.

In line with the analysis above, the reason ${}^{2h}K(F1,F2)$ coupling in FH...FH has a small value can also be explained. In addition to the partial cancellation of the three leading terms, it can be observed from Table 2 that the remainder terms have very small values for FH...FH, while they are significant for all other complexes of the series. This trend can be explained on the following basis. The orbital energy associated with LP(F2) (that is, the orbital energy of the canonical MO mostly associated with LP(F2)) is more negative than those of LP(N2) and LP(O2) (approximately, they scale as *Z*, the atomic number). Therefore, virtual excitations LP(F2) \rightarrow (vacant LMOs) are more hindered than for other kind of lone pairs. This means that the perturbed LP(F2) LMO has smaller contributions from vacant LMOs of the F1 environment than LP(O2) or LP(N2) ones and, consequently, it is less efficient to transmit the spin information. This fact can be verified, for instance, noticing that PP terms which

TABLE 5: Main ${}^{2h}K_{ia,jb}$ Coupling Pathways for All Complexes Considered^a (All Values Given in $10^{19} \text{ N A}^{-2} \text{ m}^{-3}$)

| <i>i</i> | <i>a</i> * | <i>j</i> | <i>b</i> * | NCH...OH2 | NCH...NCH | NCH...FH |
|----------|------------|-------------------|------------|-----------|-----------|----------|
| LP(A) | HB* | C-H | HB* | 1.57 | 1.45 | 1.14 |
| LP(A) | HB* | C-H | C-H* | 1.00 | 0.57 | 1.04 |
| LP(A) | HB* | A-X2 ^b | HB* | 0.94 | 0.67 | <0.19 |
| LP(A) | HB* | LP(A) | HB* | 0.77 | 0.88 | 0.67 |
| <i>i</i> | <i>a</i> * | <i>j</i> | <i>b</i> * | FH...OH2 | FH...NCH | FH...FH |
| LP(A) | HB* | LP(F1) | LP(F1)* | 4.14 | 2.79 | 2.22 |
| LP(A) | HB* | LP(A) | HB* | 1.93 | 1.84 | 0.75 |
| LP(A) | HB* | A-X2 ^b | HB* | 1.08(x2) | 1.48 | 0.75 |
| LP(A) | HB* | S(F1) | LP(F1)* | -1.81 | -1.28 | -0.96 |
| LP(A) | HB* | F1-H | HB* | -1.17 | -0.72 | -0.93 |
| LP(A) | HB* | LP(A) | LP(F1)* | -1.04 | -1.17 | -0.58 |
| LP(A) | HB* | A-X2 ^b | LP(F1)* | -0.48(x2) | -0.87 | -0.60 |
| <i>i</i> | <i>a</i> * | <i>j</i> | <i>b</i> * | CNH...OH2 | CNH...NCH | CNH...FH |
| LP(A) | HB* | LP(N1) | LP(N1)* | 2.71 | 3.69 | 1.17 |
| LP(A) | HB* | LP(N1) | HB* | 2.58 | 3.36 | 2.24 |
| LP(A) | HB* | LP(A) | HB* | 1.20 | 2.29 | 1.04 |
| LP(A) | HB* | A-X2 ^b | HB* | 1.63 | 1.49 | 0.69 |
| LP(A) | HB* | LP(A) | LP(N1)* | -0.56 | -1.16 | -0.55 |
| LP(A) | HB* | S(N1) | LP(N1)* | -0.62 | -0.83 | ~0.00 |

^a *i* and *j* represent occupied LMOs, *a** and *b** represent vacant LMOs. See text for explanation of the symbols used. ^b X2 stands for the atom directly bonded to the A atom.

involve LP(F2) are smaller than similar terms which involve other type of lone pairs, yielding smaller contributions to the coupling.

The ${}^{1h}K(A,H)$ couplings have a more straightforward interpretation. From Table 3, it can be noticed that the whole coupling can be actually ascribed to a single type of K_{ij} term, namely that which involves LP(A) and D-H LMOs, while all other terms have almost negligibly small values (except $K_{LP(N2),LP(N1)}$ for CNH...NCH). However, it is remarkable that in almost all cases, $K_{LP(A),D-H}$ for 1h-couplings are of smaller absolute magnitude than similar terms for 2h-couplings. The only exception to this rule is for donor CNH, owing to the N1-H bond characteristics discussed above. The reasons of this trends must be sought in the $K_{ia,jb}$ coupling pathways behavior and will be discussed in the following section.

Four Indices ${}^{2h}K_{ia,jb}(D,A)$ and ${}^{1h}K_{ia,jb}(A,H)$ Contributions: Why ${}^{2h}K(A,D)$ s Are Larger Than ${}^{1h}K(A,H)$ s in Absolute Value. The reason for the larger absolute value of ${}^{2h}K(A,D)$ compared to ${}^{1h}K(A,H)$ can be well understood comparing their main coupling pathways $K_{ia,jb}$. In this section, a CLOPPA decomposition is presented that makes clear the role played by different occupied and vacant LMOs. In Tables 5 and 6 the main coupling pathways, ${}^{2h}K_{ia,jb}$ and ${}^{1h}K_{ia,jb}$, are displayed, respectively, for all complexes considered.

From Tables 5 and 6 it is seen that all main coupling pathways $K_{ia,jb}$ in both ${}^{2h}K(D,A)$ and ${}^{1h}K(A,H)$ involve at least one virtual excitation LP(A) \rightarrow HB*. The efficiency of these LMOs to transmit the spin information is thus shown. The second type of excitations yielding significant values are as follows: (a) excitations from occupied to vacant LMOs of the donor molecule environment, namely LP(D) \rightarrow LP(D)*, D-H \rightarrow D-H*, or to HB* LMOs, i.e., LP(D) \rightarrow HB* or D-H \rightarrow HB*, and (b) virtual excitations from occupied LMOs of the acceptor molecule environment to HB* or to LP(D)*. For the first type, path a, the magnitude of the coupling pathways is essentially due to the product of two large perturbators, each one at the site of each coupled nucleus A and D, or A and H (see eq 3). For the latter, path b, perturbators have significant values on

TABLE 6: Main ${}^1\text{h}K_{ia,jb}$ Coupling Pathways for All Complexes Considered^a (All Values Given in $10^{19} \text{ N A}^{-2} \text{ m}^{-3}$)

| <i>i</i> | <i>a</i> * | <i>j</i> | <i>b</i> * | NCH...OH2 | NCH...NCH | NCH...FH |
|----------|------------|----------|------------|-----------|-----------|----------|
| LP(A) | HB* | C-H | C-H* | -0.66 | -0.60 | -0.48 |
| LP(A) | HB* | C-H | HB* | -0.15 | 0.05 | -0.12 |
| <i>i</i> | <i>a</i> * | <i>j</i> | <i>b</i> * | FH...OH2 | FH...NCH | FH...FH |
| LP(A) | HB* | F1-H | HB* | -0.90 | -0.62 | -0.74 |
| LP(A) | HB* | F1-H | F1-H* | -0.84 | -0.66 | -0.50 |
| <i>i</i> | <i>a</i> * | <i>j</i> | <i>b</i> * | CNH...OH2 | CNH...NCH | CNH...FH |
| LP(A) | HB* | N1-H | HB* | -0.65 | -0.48 | -0.42 |
| LP(A) | HB* | N1-H | N1-H* | -0.38 | -0.45 | 0.24 |

^a *i* and *j* represent occupied LMOs, *a** and *b** represent vacant LMOs. See text for explanation of the symbols used.

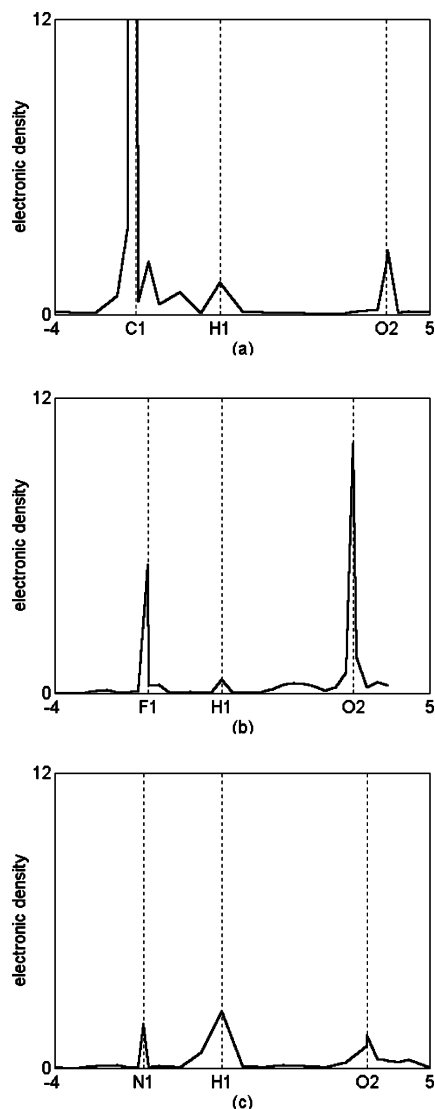


Figure 3. Plot of the electronic density (in au) of HB* LMOs in the complexes (a) NCH...OH₂, (b) FH...OH₂, and (c) CNH...OH₂. Vacant LMOs concentrated around the O2 atom are excluded from the calculation, to enhance the appreciation of peaks in D and H.

both nuclei A and D, but only small values on the H nucleus. The former is basically the type of coupling pathways which give rise to ${}^1\text{h}K(\text{A,H})$. In fact, the whole coupling is essentially defined by two coupling pathways involving D-H → HB* and D-H → D-H*. These contributions to ${}^1\text{h}K(\text{A,H})$ are comparable to the similar coupling pathways in ${}^2\text{h}K(\text{D,A})$. Hence, the

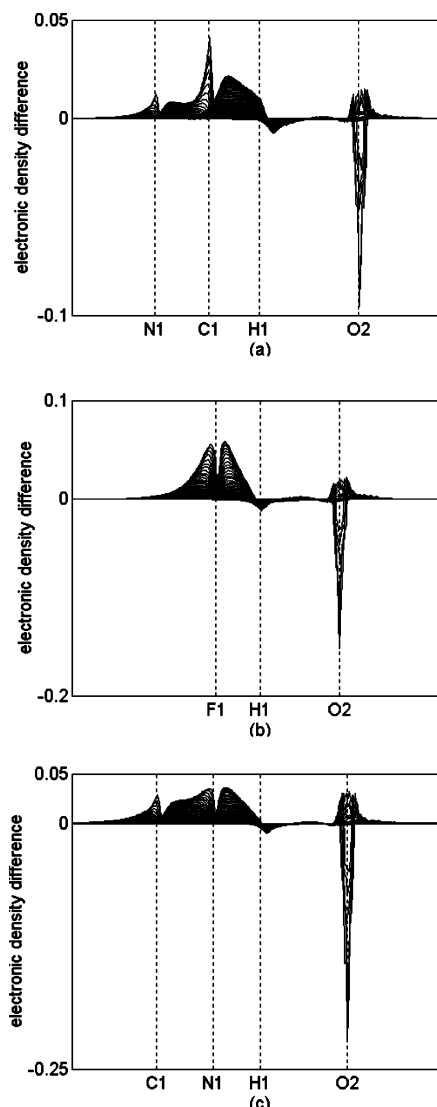


Figure 4. Plot of the electronic density difference (in au) of LP(O2) in the complexes and in the OH₂ isolated molecules. Values of the ordinate axis are rescaled in order to appreciate better the difference in shape. Key: (a) NCH...OH₂; (b) FH...OH₂; (c) CNH...OH₂.

fact that ${}^1\text{h}K(\text{A,H})$ values are much smaller than ${}^2\text{h}K(\text{D,A})$ (except, as it was just analyzed, for FH...FH) can be explained taking into account that, for ${}^2\text{h}K(\text{D,A})$, (i) other path a type excitations, like LP(D) → LP(D)* are very efficient to transmit the spin information, as it presents large perturbators at the D site, and (ii) both types of coupling pathways, a and b, contribute efficiently to the coupling, (despite many compensations, as it was explained for ${}^2\text{h}K(\text{F1,A})$). The reason no terms of the b type contribute to ${}^1\text{h}K(\text{A,H})$ can be well understood by analyzing, for instance, the coupling pathway which involves twice the LP(A) → HB* excitation. This term is included among the most important ones for ${}^2\text{h}K(\text{D,A})$, while it has a negligibly small value for ${}^1\text{h}K(\text{A,H})$. It must be kept in mind that, for given indices *i,a,j,b* the propagator element $P_{ia,jb}$ is the same for both couplings and, therefore the difference in the values of the corresponding coupling pathway $J_{ia,jb}$ depends on the perturbators V_{ia} and V_{jb} at each nucleus. Hence, the difference between this coupling pathway for both couplings can be ascribed to the characteristics of the HB* and LP(A) LMOs. On one hand, HB* LMOs, in most cases, present high peaks around the D and A sites, but only a small one in H. Figure 3 depicts these characteristics of HB* LMOs in three examples. As was

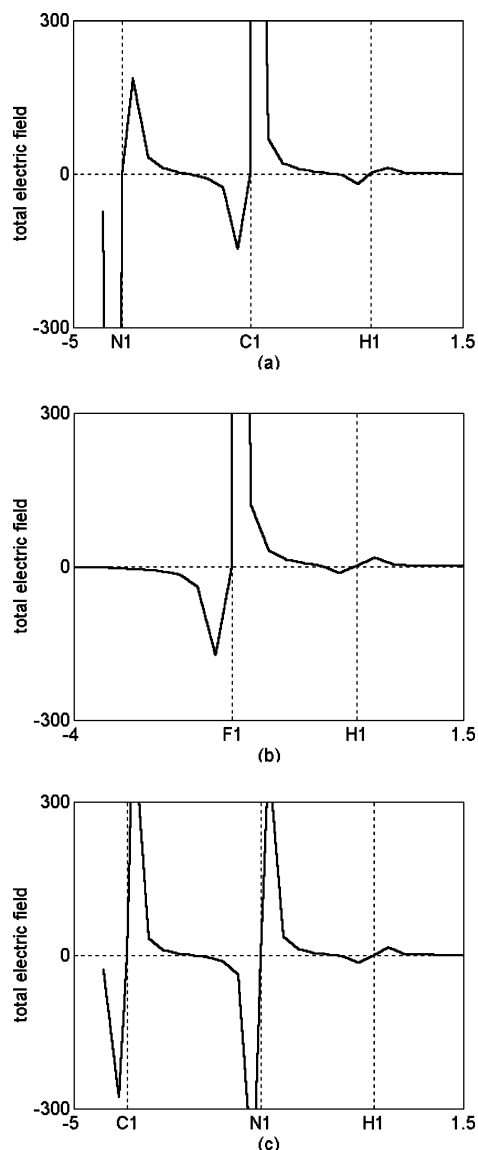


Figure 5. Plot of the total electric field (in au) of the isolated donor molecules vs the position in the molecule region. Key: (a) NCH; (b) FH; (c) CNH.

mentioned in the preceding section, it is seen that the s-character of HB^* LMOs at the D site is smaller for D centers bearing “anti lone pairs” LP(D)^* . The HB^* density presents a huge peak in C1, (Figure 3a), with the characteristic of an “anti lone pair” LMO, a smaller, although still significant, density on F1 (Figure 3b), and only a rather small peak in N1 (Figure 3c).

On the other hand, the way LP(A) is delocalized over the donor environment is crucial to determine the role of this LMO in ${}^2\text{hK(A,D)}$ and ${}^1\text{hK(A,H)}$.

Parts a–c of Figure 4 show the difference of density between unperturbed LP(A) LMO in the complexes and in the isolated molecules, in the case of a H_2O acceptor. As it can be expected, as a consequence of the attractive interaction yielding a hydrogen bond of type $\text{D-H}\cdots\text{A}$, the sp-type A lone pair, LP(A) , extends toward the D and H nuclei, decreasing its density at the A site. It is interesting to note that the LP(A) “tail” density shape at the donor site closely resembles the D–H density one. This fact shows the way that LMOs from one molecule mix to LMOs from the other, to form a complex. This fact is in qualitative agreement with the PMO theory,⁵⁵ and it is well reproduced by the localization technique. However, Figure 4 also exhibits a significant difference that distinguishes the LP(A) “tail” density

shape from a D–H electronic density: there is a decreasing of the density at the H site from the corresponding one of a D–H LMO. In fact, in Figure 4 it is observed that density at the H site does not present the characteristic peak of a D–H bond, but a small value which, in the case of $\text{FH}\cdots\text{OH}_2$, is almost null. This rather unexpected feature is the reason, even though LP(A) extends over the D–H region, it is inefficient to transmit the spin information at the H nucleus. This characteristic of the magnetically unperturbed LP(A) LMO is determined by its interaction with the donor molecule upon complex formation. It can be explained analyzing the electric field of the donor molecule at its own region, that is the field that the LP(A) LMO feels as it is coming closer to the donor molecule. Figure 5 shows the characteristics of these fields for the isolated donor molecules.

From Figure 5, it can be observed that the electric field values around each nucleus are such that a concentration of electronic charge is favored. However, the electric field values around the H nucleus are so much smaller than the corresponding ones around the other nuclei, that only a small density of electronic charge could be expected in that zone. Therefore, the charge transfer from LP(A) to the donor molecule region is mainly localized around the D nucleus. This fact makes perturbators $\text{LP(A)} \rightarrow \text{HB}^*$ to have a considerable large value in D and a negligibly small one in H. As this excitation is present in all main coupling pathways, the corresponding (absolute) values are larger for 2h-couplings than for 1h-ones.

As a final remark, the role played by the HB^* vacant LMO shows that this type of couplings is different from “through-space” couplings, for which the main coupling pathways involve two excitations where the occupied and vacant LMOs involved belong both to each coupled nucleus environment.⁴⁰

Concluding Remarks

The CLOPPA decomposition of J couplings in contributions of local fragments is a useful tool to analyze the electronic mechanisms that are taking place and to characterize their behavior in different molecular environments. Moreover, it can be expected that results thus obtained could be extrapolated to other phenomena under similar conditions and, in that sense, this type of analysis can be considered as predictive. The CLOPPA analysis of ${}^1\text{hK(A,H)}$ and ${}^2\text{hK(A,D)}$ in several model complexes with hydrogen bonds of the type $\text{D-H}\cdots\text{A}$ allowed to explain the electronic origin of the main coupling mechanisms involved. Besides, this type of analysis led to an explanation of the larger absolute value of the 2h-coupling than the 1h-one in terms of LMOs within the local $\text{D-H}\cdots\text{A}$ fragment. In particular, the crucial role of vacant LMOs localized in the bridge zone and their interaction with the acceptor atom lone pair, LP(A) , is demonstrated.

Acknowledgment. Financial support from UBACYT and CONICET is gratefully acknowledged. We would like to thank Prof. P. Lazeretti for providing us a copy of the SYSMO program.

References and Notes

- (1) Dingley, A. J.; Grzesiek, S. *J. Am. Chem. Soc.* **1998**, *120*, 8293.
- (2) Dingley, A. J.; Masse, J. E.; Peterson, R. D.; Barfield, M.; Feigon, J.; Grzesiek, S. *J. Am. Chem. Soc.* **1999**, *121*, 6019.
- (3) Cordier, F.; Rogowski, M.; Grzesiek, S.; Bax, A. *J. Magn. Reson.* **1999**, *140*, 510.
- (4) Wang, Y. X.; Jacob, J.; Cordier, F.; Wingfield, P.; Stahl, S. J.; Lee-Huang, S.; Torchia, D.; Grzesiek, S.; Bax, A. *J. Biomol. NMR* **1999**, *14*, 181.
- (5) Cornilescu, G.; Hu, J.; Bax, A. *J. Am. Chem. Soc.* **1999**, *121*, 2949.

- (6) Cornilescu, G.; Ramirez, B. E.; Frank, M. K.; Clore, G. M.; Gronenborn, A. M.; Bax, A. *J. Am. Chem. Soc.* **1999**, *121*, 6275.
- (7) Golubev, N. S.; Shenderovich, I. G.; Smirnov, S. N.; Denisov, G. S.; Limbach, H. H. *Chem.—Eur. J.* **1999**, *5*, 492.
- (8) Case, D. A. *Curr. Opin. Struct. Biol.* **2000**, *10*, 197.
- (9) Meissner, A.; Sørensen, O. W. *J. Magn. Reson.* **2000**, *143*, 387.
- (10) Scheurer, C.; Brüschweiler, R. *J. Am. Chem. Soc.* **1999**, *121*, 8661.
- (11) Del Bene, J. E. *J. Am. Chem. Soc.* **2000**, *122*, 3560.
- (12) Del Bene, J. E.; Bartlett, R. J. *J. Am. Chem. Soc.* **2000**, *122*, 10480.
- (13) Benedict, H.; Shenderovich, I. G.; Malkina, O. L.; Malkin, V. G.; Denisov, G. S.; Golubev, N. S.; Limbach, H. H. *J. Am. Chem. Soc.* **2000**, *122*, 1979.
- (14) Pecul, M.; Leszczynski, J.; Sadlej, J. *J. Chem. Phys.* **2000**, *112*, 7930.
- (15) Pecul, M.; Leszczynski, J.; Sadlej, J. *J. Phys. Chem. A* **2000**, *104*, 8105.
- (16) Del Bene, J. E.; Perera, S. A.; Bartlett, R. J. *J. Phys. Chem. A* **2001**, *105*, 930.
- (17) Del Bene, J. E.; Jordan, M. J. T. *J. Mol. Struct. (THEOCHEM)* **2001**, *11*, 573.
- (18) Jordan, M. J. T.; Toh, J. S.-S.; Del Bene, J. E. *Chem. Phys. Lett.* **2001**, *346*, 288.
- (19) Toh, J. S.-S.; Jordan, M. J. T.; Husowitz, B. C.; Del Bene, J. E. *J. Phys. Chem.* **2001**, *105*, 10906.
- (20) Del Bene, J. E.; Perera, S. A.; Bartlett, R. J. *Magn. Reson. Chem.* **2001**, *39*, S109.
- (21) Pecul, M.; Sadlej, J.; Leszczynski, J. *J. Chem. Phys.* **2001**, *115*, 5498.
- (22) Barfield, M.; Dingley, A. J.; Feigon, J.; Grzesiek, S. *J. Am. Chem. Soc.* **2001**, *123*, 4014.
- (23) Pecul, M.; Sadlej, J. *Chem. Phys. Lett.* **2002**, *360*, 272.
- (24) Del Bene, J. E.; Bartlett, R. J.; Elguero, J. *Magn. Reson. Chem.* **2002**, *40*, 767.
- (25) Giribet, C. G.; Ruiz de Azúa, M. C.; Vizioli, C. V.; Cavasotto, C. N. *Int. J. Mol. Sci.* **2003**, *4*, 203.
- (26) Wilkens, S. J.; Westler, W. M.; Weinhold, F.; Markley, J. L. *J. Am. Chem. Soc.* **2002**, *124*, 1190.
- (27) Del Bene, J. E.; Perera, S. A.; Bartlett, R. J.; Yáñez, M.; Mó, O.; Elguero, J.; Alkorta, I. *J. Phys. Chem. A* **2003**, *107*, 3222.
- (28) Del Bene, J. E.; Perera, S. A.; Bartlett, R. J.; Yáñez, M.; Mó, O.; Elguero, J.; Alkorta, I. *J. Phys. Chem. A* **2003**, *107*, 3121.
- (29) Alkorta, I.; Elguero, J. *Int. J. Mol. Sci.* **2003**, *4*, 64.
- (30) Del Bene, J. E.; Elguero, J. *Chem. Phys. Lett.* **2003**, *382*, 100.
- (31) Pecul, M.; Sadlej, J.; Helgaker, T. *Chem. Phys. Lett.* **2003**, *372*, 476.
- (32) Del Bene, J. E.; Elguero, J.; Alkorta, I.; Yáñez, M.; Mó, O. *J. Chem. Phys.* **2004**, *120*, 3237.
- (33) Tuttle, T.; Kraka, E.; Wu, A.; Cremer, D. *J. Am. Chem. Soc.* **2004**, *126*, 5093.
- (34) Del Bene, J. E. *J. Phys. Chem. A* **2004**, *108*, 6820.
- (35) Tuttle, T.; Gräfenstein, J.; Wu, A.; Kraka, E.; Cremer, D. *J. Phys. Chem. B* **2004**, *108*, 1115.
- (36) Del Bene, J. E.; Elguero, J. *Magn. Reson. Chem.* **2004**, *42*, 421.
- (37) Fukui, H.; Baba, T. *Specialist Periodical Reports: Nuclear Magnetic Resonance*; Royal Society of Chemistry: London, 2000; Vol. 30, p 109.
- (38) Engelmann, A. R.; Contreras, R. H. *Int. J. Quantum Chem.* **1983**, *23*, 1033.
- (39) Ruiz de Azúa, M. C.; Diz, A. C.; Giribet, C. G.; Contreras, R. H.; Rae, I. D. *Int. J. Quantum Chem.* **1986**, *S20*, 585.
- (40) Diz, A. C.; Giribet, C. G.; Ruiz de Azúa, M. C.; Contreras, R. H. *Int. J. Quantum Chem.* **1990**, *37*, 663.
- (41) Ruiz de Azúa, M. C.; Giribet, C. G.; Vizioli, C. V.; Contreras, R. H. *J. Mol. Struct. (THEOCHEM)* **1998**, *433*, 141.
- (42) Giribet, C. G.; Ruiz de Azúa, M. C.; Gómez, S. B.; Botek, E. L.; Contreras, R. H.; Adcock, W.; Della, E. W.; Krstic, A. R.; Lochert, I. *J. Comput. Chem.* **1998**, *19*, 181.
- (43) Giribet, C. G.; Demarco, M. D.; Ruiz de Azúa, M. C.; Contreras, R. H. *Mol. Phys.* **1997**, *91*, 105.
- (44) Lazzaretto, P.; Malagoli, M.; Zanasi, R.; Della, E. W.; Lochert, I. J.; Giribet, C. G.; Ruiz de Azúa, M. C.; Contreras, R. H. *J. Chem. Soc., Faraday Trans.* **1998**, *91*, 4031.
- (45) Jørgensen, P.; Simons, J. *Second Quantization-based Methods in Quantum Chemistry*; Academic Press: London, 1981.
- (46) Geertsen, J.; Oddershede, J. *Chem. Phys.* **1984**, *90*, 301.
- (47) Enevoldsen, T.; Oddershede, J.; Sauer, S. P. A. *Theor. Chim. Acc.* **1998**, *100*, 275.
- (48) Scuseria, G. E.; Contreras, R. H. *Int. J. Quantum Chem.* **1983**, *S20*, 603.
- (49) *Gaussian 98, Revision A.7*: Frisch, M. J.; Trucks, G. W.; Schlegel, H. B.; Scuseria, G. E.; Robb, M. A.; Cheeseman, J. R.; Zakrzewski, V. G.; Montgomery, J. A.; Stratmann, R. E., Jr.; Burant, J. C.; Dapprich, S.; Millam, J. M.; Daniels, A. D.; Kudin, K. N.; Strain, M. C.; Farkas, O.; Tomasi, J.; Barone, V.; Cossi, M.; Cammi, R.; Mennucci, B.; Pomelli, C.; Adamo, C.; Clifford, S.; Ochterski, J.; Petersson, G. A.; Ayala, P. Y.; Cui, Q.; Morokuma, K.; Malick, D. K.; Rabuck, A. D.; Raghavachari, K.; Foresman, J. B.; Cioslowski, J.; Ortiz, J. V.; Baboul, A. G.; Stefanov, B. B.; Liu, G.; Liashenko, A.; Piskorz, P.; Komaromi, I.; Gomperts, R.; Martin, R. L.; Fox, D. J.; Keith, T.; Al-Laham, M. A.; Peng, C. Y.; Nanayakkara, A.; Gonzalez, C.; Challacombe, M.; Gill, P. M. W.; Johnson, B.; Chen, W.; Wong, M. W.; Andres, J. L.; Gonzalez, C.; Head-Gordon, M.; Replogle, E. S.; Pople, J. A. *Gaussian, Inc.*: Pittsburgh, PA, 1998.
- (50) Lazzaretto, P.; Zanasi, R. *J. Chem. Phys.* **1982**, *77*, 2448.
- (51) Lazzaretto, P. *Int. J. Quantum Chem.* **1979**, *15*, 181.
- (52) Lazzaretto, P. *J. Chem. Phys.* **1979**, *71*, 2514.
- (53) *DALTON, a Molecular Electronic Structure Program, Release I.2*: Helgaker, T.; Jensen, H. J. Aa.; Jørgensen, P.; Olsen, J.; Ruud, K.; Ågren, H.; Auer, A. A.; Bak, K. L.; Bakken, V.; Christiansen, O.; Coriani, S.; Dahle, P.; Dalskov, E. K.; Enevoldsen, T.; Fernandez, B.; Hättig, C.; Hald, K.; Halkier, A.; Heiberg, H.; Hetttema, H.; Jonsson, D.; Kirpekar, S.; Kobayashi, R.; Koch, H.; Mikkelsen, K. V.; Norman, P.; Packer, M. J.; Pedersen, T. B.; Ruden, T. A.; Sanchez, A.; Saue, T.; Sauer, S. P. A.; Schimmelpfennig, B.; Sylvester-Hvid, K. O.; Taylor, P. R.; Vahtras, O. 2001.
- (54) Van Duijneveldt, F. B. *IBM Res. Rep.* **1971**, RJ 945.
- (55) Dewar, M. J. S.; Dougherty, R. C. *The PMO Theory of Organic Chemistry*; Plenum Press: New York, 1975.